Supporting Information

Understanding alkali cation regulation of oxygen evolution on nickel (oxy)hydroxide

Yi Wei[a], Ling Li[a], Miao Fan[a], Jinyan Xiong[b], Weijie Li[c], and Chao Han[a]*

[a].School of Materials Science and Engineering, Central South University, Changsha 410083, P. R. China.

[b].College of Chemistry and Chemical Engineering, Wuhan Textile University, Wuhan 430200, P. R. China.

[c].Powder Metallurgy Research Institute, Central South University, Changsha 410083, P. R. China.

E-mail: Chaohan@csu.edu.cn (Corresponding author: Chao Han).

Experimental section

Materials Preparation.

The flower shaped NiO_xH_y microsphere is synthesized by a simple hydrothermal method. Typically, 1 mmol nickel chloride hexahydrate, 10 mmol urea, and 5 mmol ammonium fluoride are added into 60 mL DI water and stirred until the homogeneous solution was formed. Subsequently, the solution was transferred into a 100 mL Teflon-lined autoclave and heated in an electric oven at 120 °C for 4 h. After cooling down to room temperature, the precipitate was collected by centrifugation and washed 3 times each with both deionized water and ethanol, and then dried at 60 °C for 12 h for further characterization and use. The purity of nickel chloride hexahydrate, lithium hydroxide, sodium hydroxide, and potassium hydroxide chemicals are all in electronic grade from Aladdin® Scientific.

Characterization.

Powder X-ray diffraction (XRD) data were recorded using a Rigaku Smartlab diffractometer with Cu-Kα (0.15406 nm) operated at 40 kV and 40 mA at a scan rate of 4° min^{-1}. X-ray photoelectron spectroscopy (XPS) analyses were operated with an AXIS-NOVA (Kratos) X-ray photoelectron spectrometer using a monochromated Al Ka X-ray source (hv = 1486.6 eV) operated at 150 W under a base pressure of 2.6 x 10^{-9} Torr. Binding energies were calibrated by setting C 1s peak to 284.6 eV. The XPS spectra were deconvoluted using the curve fitting program, CasaXPS. The scanning electron microscopy (SEM) images were obtained using a Hitachi S-4800 microscope operated at an acceleration voltage of 10 kV. The transmission electron microscope (TEM), high-resolution transmission electron microscope (HR-TEM) and scanning TEM (STEM), as well as EDS spectra and elemental mapping, were obtained using a Hitachi HF-3300. Raman spectroscopy was recorded on the Renishaw inVia Raman microscope under an excitation of 532 nm laser under controlled potentials by a potentiostat (Gamry interface 1010). The electrolytic cell was homemade by quartz glass as the cover to protect the objective. The working electrode was set to keep the plane of the sample perpendicular to the incident laser. Pt wire as the counter electrode, and $Ag/AgCl_{(sat.\ KCl)}$ as reference electrolyte. In-situ attenuated reflection-surface enhanced infrared absorption spectroscopy (ATR-SEIRAS) was recored on PerkinElmer spectrometers.

Electrochemical measurements.

The electrochemical characterizations were carried out with a potentiostat (Gamry Interface 1010) at room temperature in alkaline electrolyte using a three-electrode configuration with Pt wire as the counter electrode, an Ag/AgCl (saturated KCl) as the reference electrode and a glassy carbon (3 mm) loaded with catalyst as the working electrode. 5 mg of catalyst was added into 800 μL deionized water,175 μL isopropanol, and 25 μL 5wt% Nafion mixed under ultrasonic dispersion for 20 mins. Then, the 2 μL suspension was dropped on a glassy carbon electrode and slowly dried. The pH values of all the alkaline solution (LiOH, NaOH and KOH) are 13.0. The cyclic voltammetry (CV) curves were recorded with a scan rate of 20 mV s^{-1} in Ar-saturated alkaline electrolyte. The electrochemical impedance spectroscopy (EIS) measurements were carried out in the frequency range of 100 kHz to 0.1 Hz. Double-layer capacitance (C_{dl}) was calculated by performing CV measurements at different scan rates of 20, 40, 60, 80 and 100 mV s^{-1} in the potential range of 0.977 - 1.077 V (vs RHE). The value of C_{dl} was obtained from plotting $\Delta j = j_a - j_c$ at 1.027 V vs RHE against the scan rates (j_a and j_c are anode and cathode current density, respectively).

Calculated Condition(Method):

All calculations were performed with the plane-wave DFT method as implemented in the Vienna ab initio simulation package (VASP). The projector augmented wave (PAW) method was used to describe the core and valence electrons. The Perdew–Burke–Ernzerhof (PBE) form of the generalized gradient approximation was employed to describe electron exchange and correlation. Calculations proceed by a 2 × 2 Ni(core shell) supercell with periodic boundary conditions. A kinetic energy cutoff of 600 eV was set in all structural relaxation simulations and the convergence criterion for the electronic self-consistent iteration is set to 10^{-5} eV. A gamma centered 6 × 6 × 1 k-point mesh was used for the Brillouin zone. In all cases, structural relaxations were performed using a conjugate gradient algorithm until forces on all atoms were below 0.01 eV/Å. All calculations were performed with spin polarization.

$$Ni + MOH \rightarrow NiM + OH$$

$$NiM + H_2O \rightarrow NiMOH + 1/2H_2$$

$$NiMOH \rightarrow NiMO + 1/2H_2$$

$$NiMO + H_2O \rightarrow NiOOHM + 1/2H_2$$

$$NiOOHM + OH \rightarrow NiM(O_2) + H_2O$$

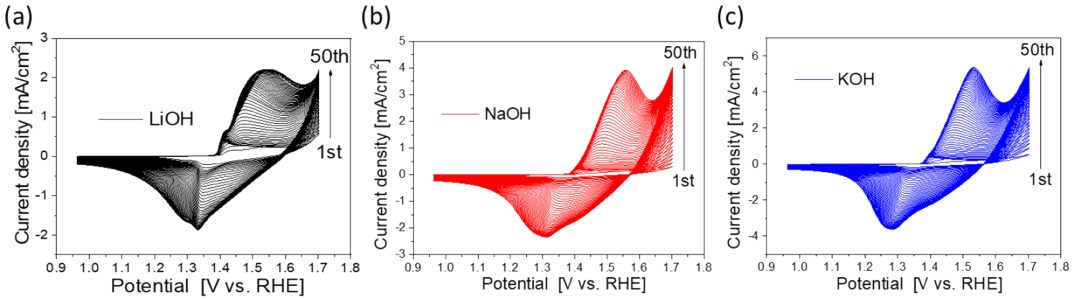

Figure S1. The initial CV activation curves of NiO_xH_y at the scan rate of 20 mV s^{-1} in (a) LiOH, (b) NaOH, and (c) KOH.

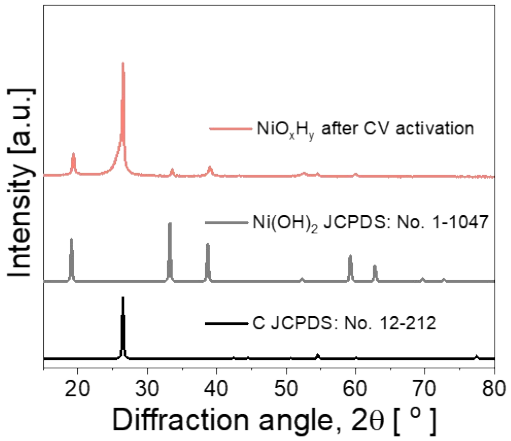

Figure S2. XRD patterns of NiO_xH_y after CV cycles in KOH electrolyte. The sample was loaded on carbon paper for XRD measurement.

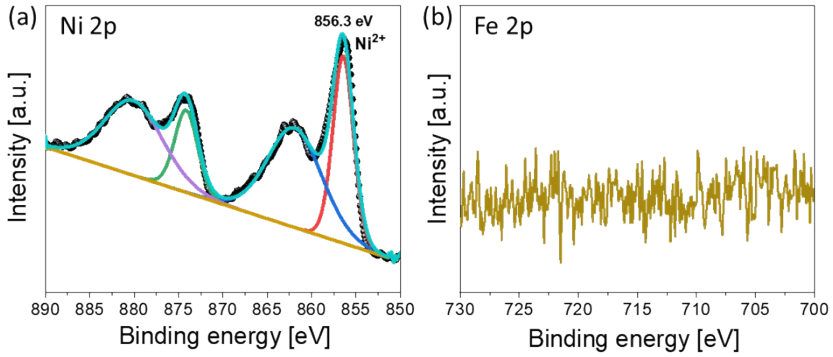

Figure S3. XPS spectra of (a) Ni 2p and (b) Fe 2p from NiO_xH_y after CV cycles in KOH electrolyte.

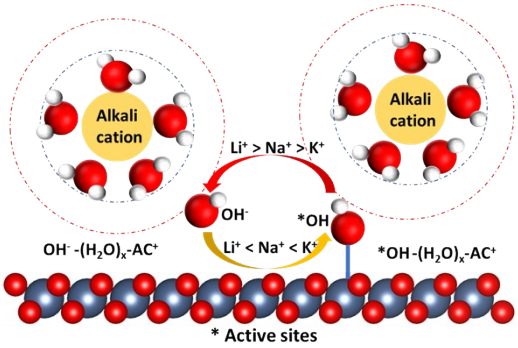

Figure S4. Illustration of alkali cation impact on *OH formation from OH^-.

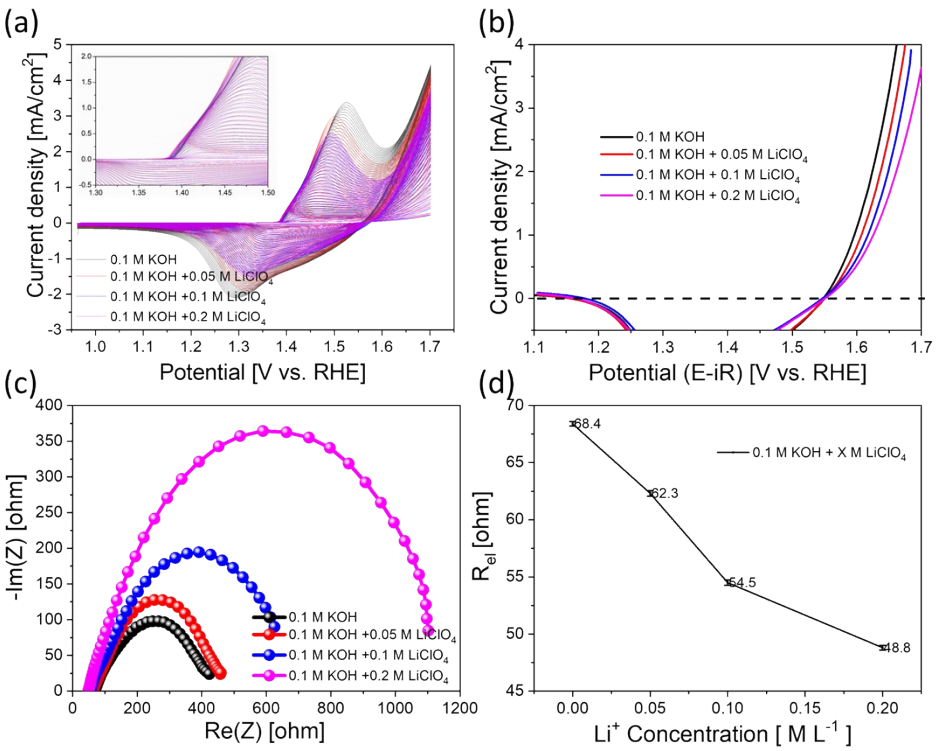

Figure S5. (a) CV curves of NiO_xH_y (b) backward CV, (c) EIS spectra (at 1.75 V vs RHE) of NiO_xH_y measured in 0.1 M KOH with different concentration of $LiClO_4$, (d) electrolyte resistances obtained from EIS spectra.

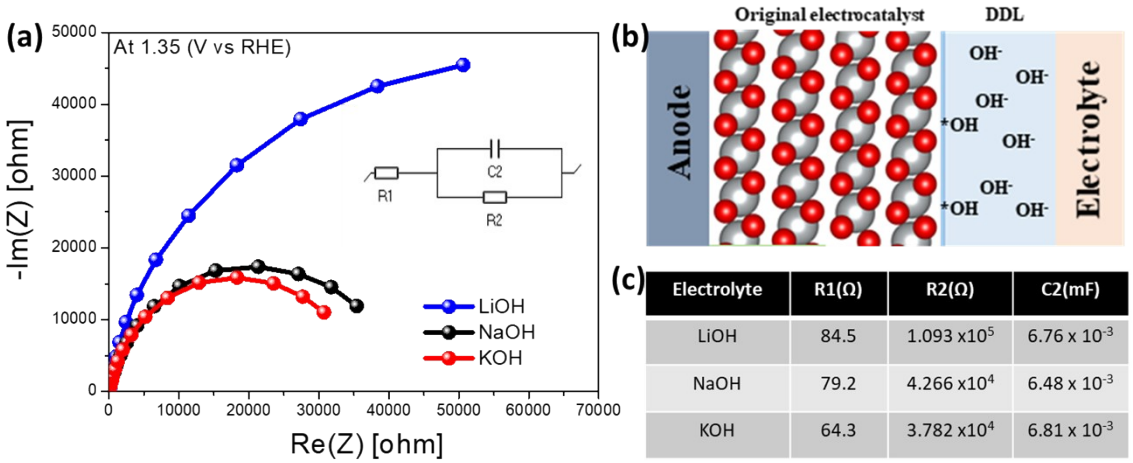

(c)

Electrolyte	R1(Ω)	R2(Ω)	C2(mF)
LiOH	84.5	1.093×10^5	6.76×10^{-3}
NaOH	79.2	4.266×10^4	6.48×10^{-3}
KOH	64.3	3.782×10^4	6.81×10^{-3}

Figure S6. (a) EIS spectra of NiO_xH_y in different electrolyte (pH=13.0) at an applied potential of 1.35 V vs RHE (Insert: Equivalent Circuit for the obtained EIS). (b) Equivalent circuit schematic diagram for NiOOH at 1.35 V vs RHE. (c) Corresponding parameters obtained from Figure S6a.

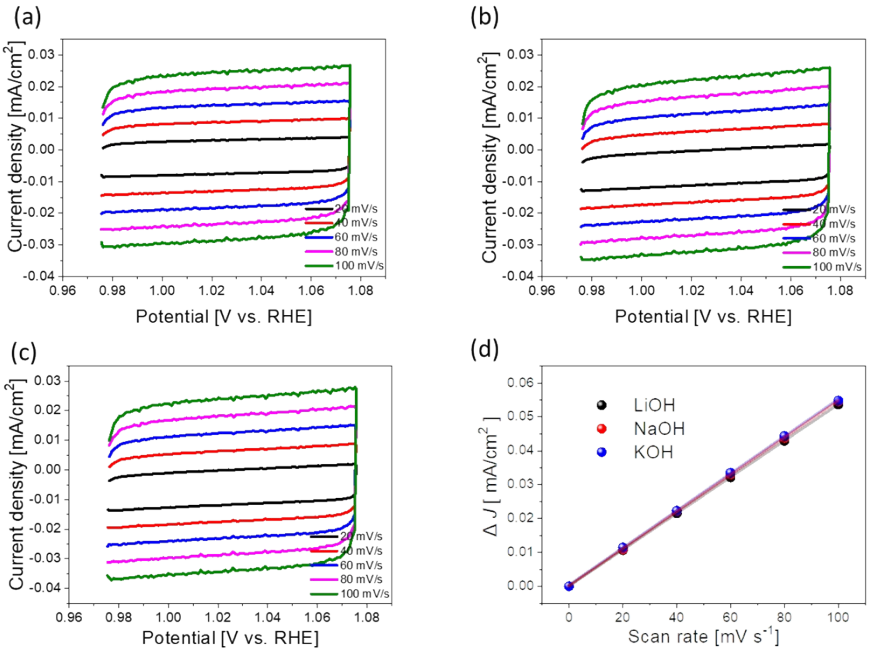

Figure S7. Typical cyclic voltammetry curves of NiO_xH_y with different scan rates in (a) LiOH, (b) NaOH, (c) KOH. (d) Plots showing the dependence of current density on the scan rate for the extraction of double layer capacitance.

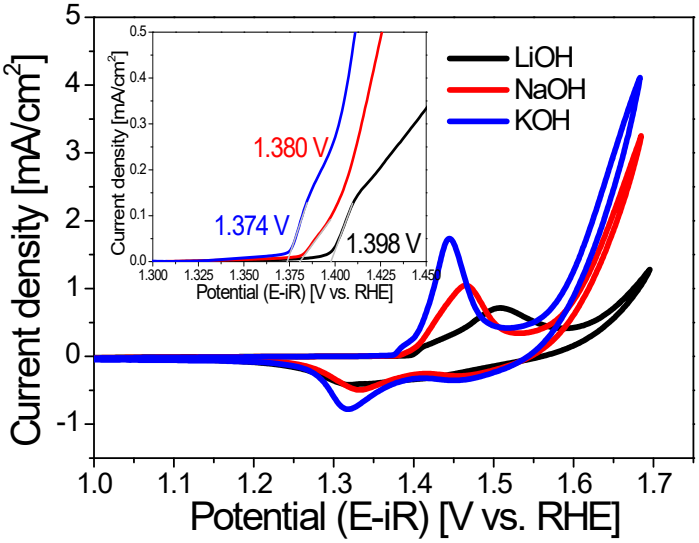

Figure S8. CV curves of NiO_xH_y at pH 13.0 in the region of oxygen evolution in different electrolytes at a scan rate of 1 mV s^{-1}.

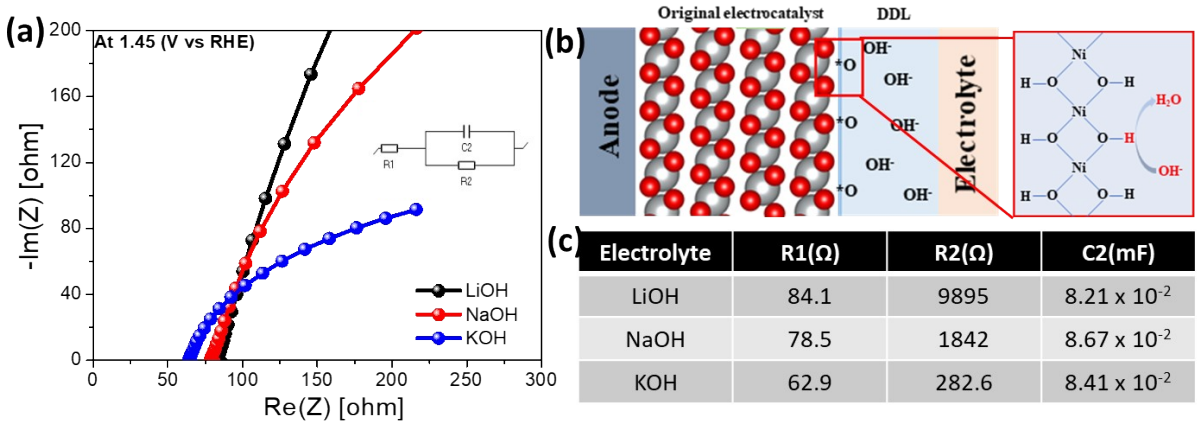

(c)

Electrolyte	R1(Ω)	R2(Ω)	C2(mF)
LiOH	84.1	9895	8.21×10^{-2}
NaOH	78.5	1842	8.67×10^{-2}
KOH	62.9	282.6	8.41×10^{-2}

Figure S9. (a) EIS spectra of NiO_xH_y in different electrolytes (pH=13.0) at an applied potential of 1.45 V vs RHE. (b) Equivalent circuit schematic diagram for NiO_xH_y at 1.45 V vs RHE (DDL: Diffusion double layer). (c) Corresponding parameters obtained from Figure S6a.

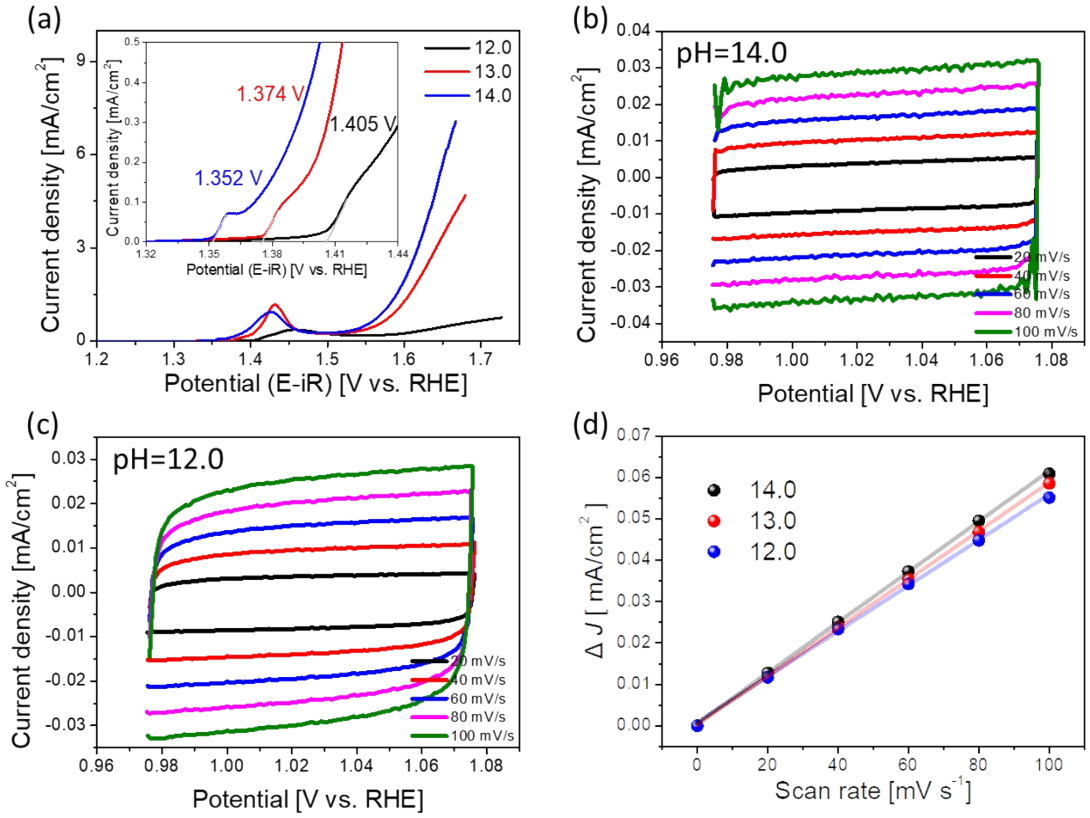

Figure S10. (a) Polarization curves of NiO_xH_y in KOH electrolyte with different pH values and activation potential of Ni^{2+} to Ni^{3+}. CV curves of NiO_xH_y at non-Faradic potential area in (b) pH =14.0 and (c) pH = 12.0 KOH electrolyte with different scan rates. (d) Plots showing the dependence of current density on the scan rate for the extraction of double layer capacitance performed on NiO_xH_y in different pH of KOH electrolyte.

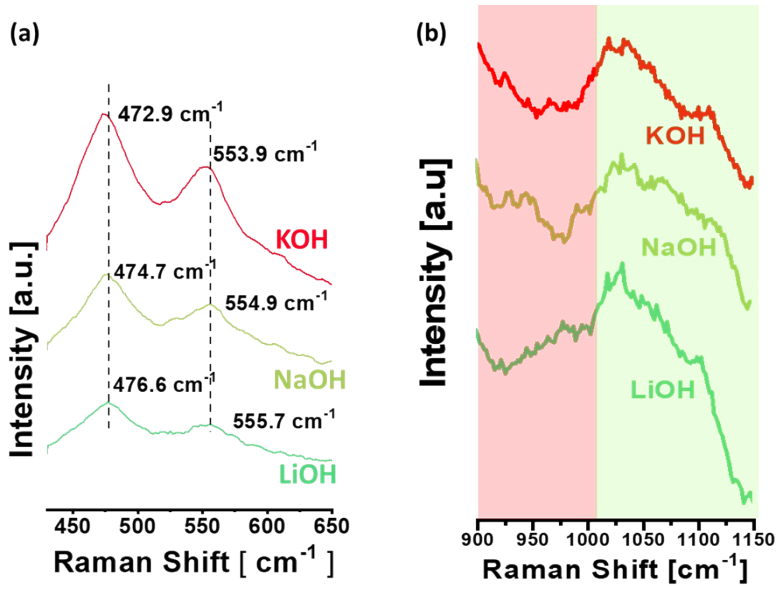

Figure S11. In-situ Raman spectra of NiO_xH_y in the wavenumber regions of (a) 430-650 cm^{-1} and (b) 900-1150 cm^{-1} acquired at 1.70 V vs RHE.

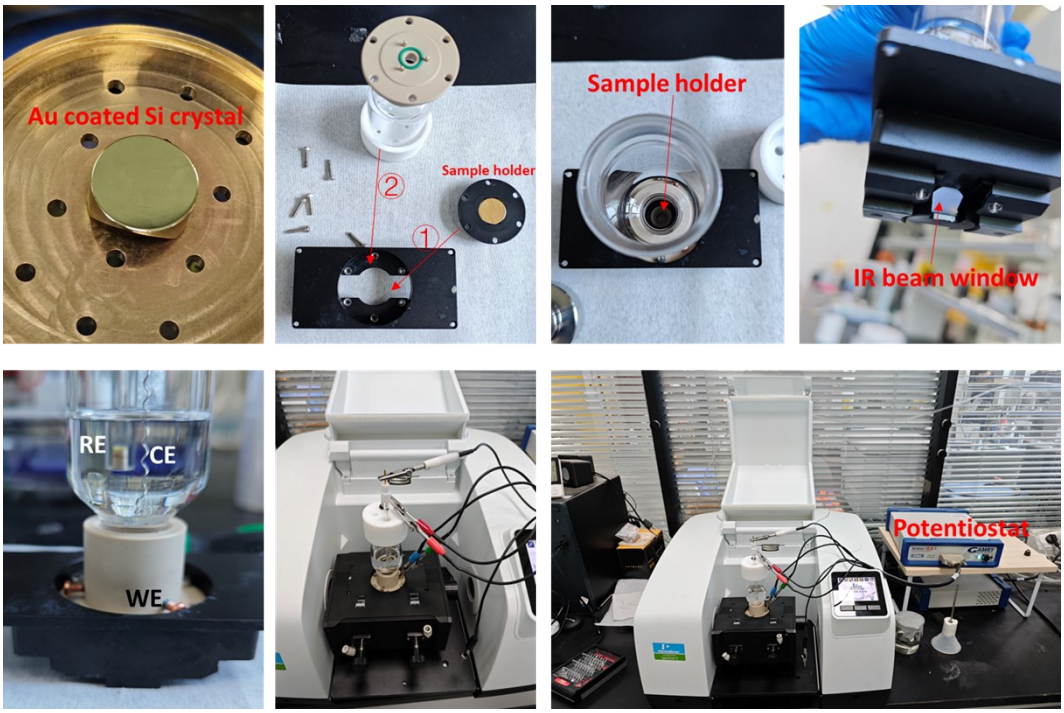

Figure S12. Photographs of in-situ ATR-SEIRAS spectra measurements.

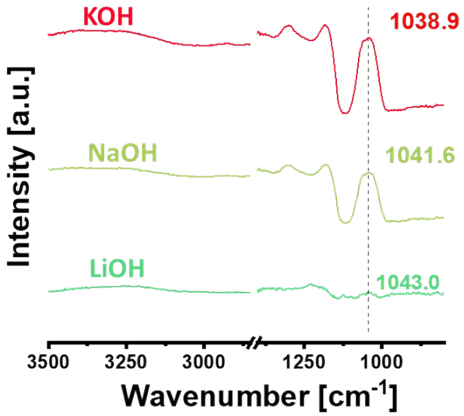

Figure S13. In-situ ATR-SEIRAS spectra of NiO_xH_y measured at 1.7 V vs RHE for 240 s.

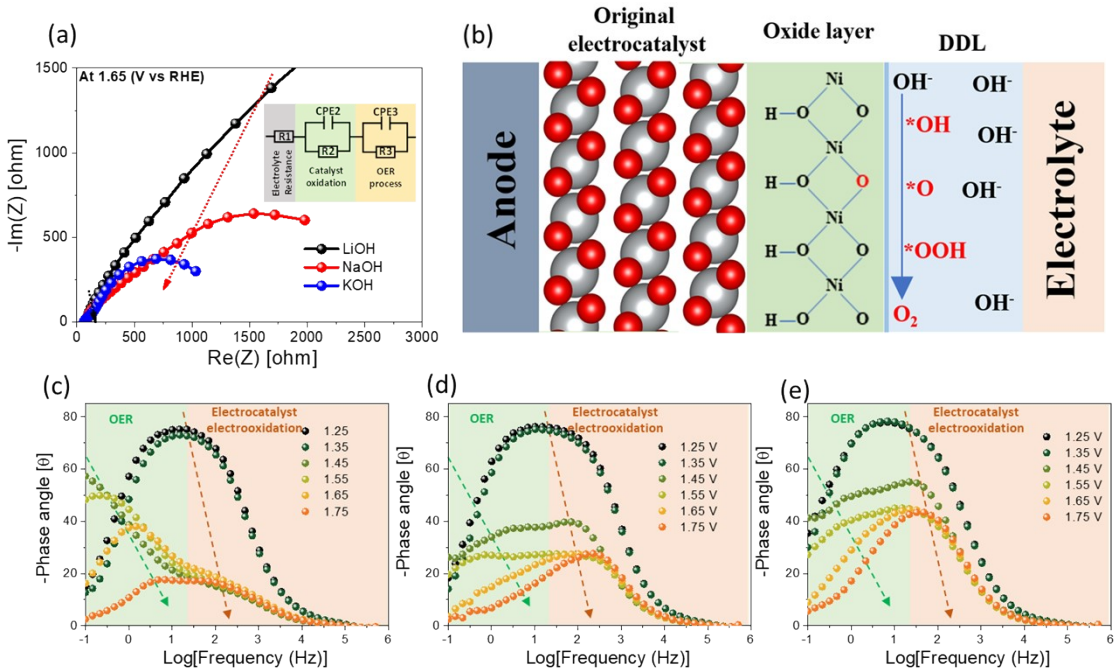

Figure S14. (a) EIS spectra of NiO_xH_y in the different electrolytes at an applied potential of 1.65 V vs RHE and the equivalent circuit insert. (b) Schematic illustration of the relationship between surface species and reactions for NiO_xH_y at a high potential range. Bode plots for NiO_xH_y at different potentials in (c) KOH, (d) NaOH, and (e) LiOH.

Table S1. Parameters obtained from Figure S14a.

Electrolyte	R1(Ω)	R2(Ω)	C2(mF)	R3(Ω)	C3(mF)
LiOH	82.4	534	0.108	6790	0.171
NaOH	80.3	234	0.066	2337	0.332
KOH	62.9	80.6	0.223	1105	0.552

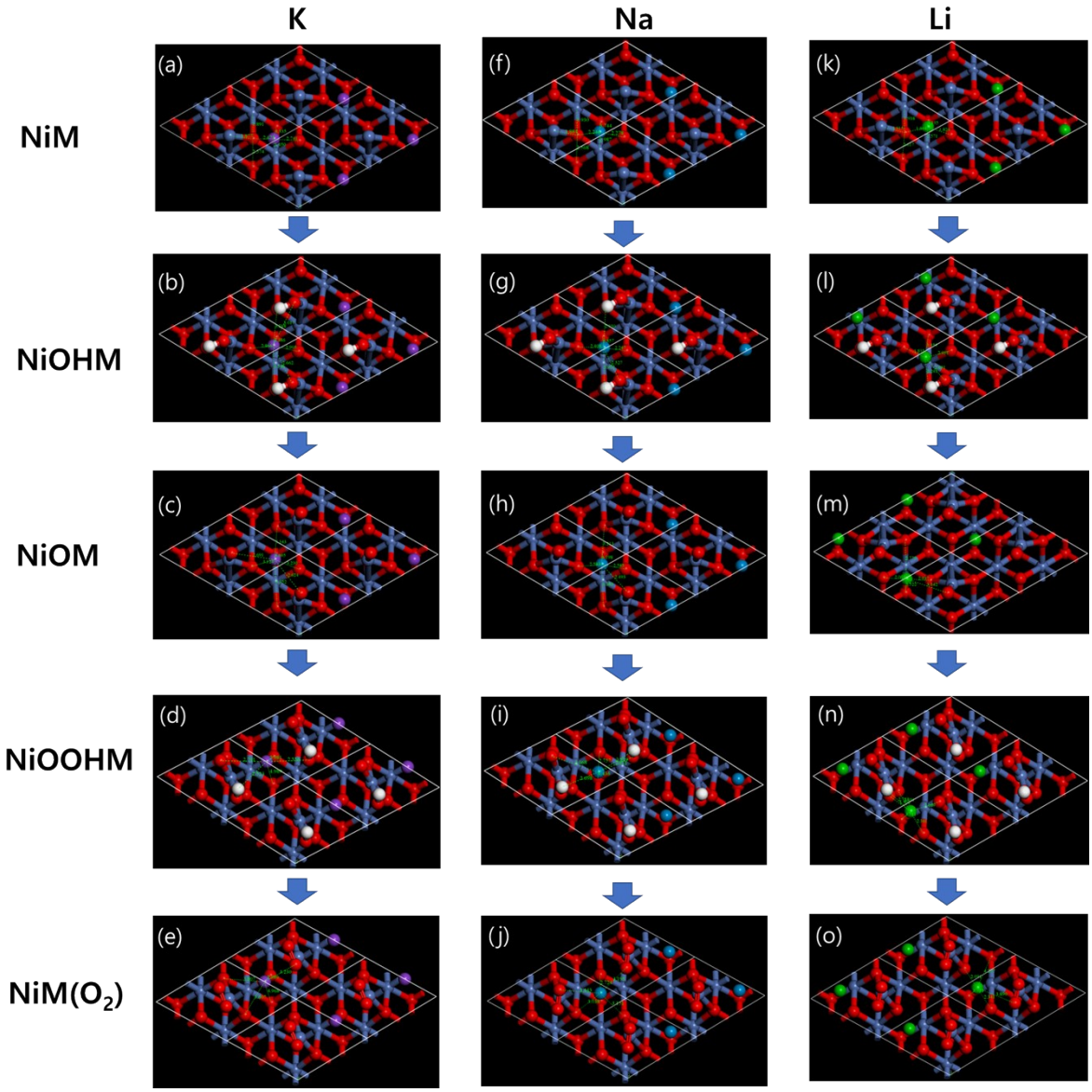

Figure S15. OER process proposed on Ni site of NiOOH with (a-e) K^+, (f-j) Na^+, (k-o) Li^+. (Ni (gray), O (red), H (white), K (purple), Na (teal), and Li (green)).

Table S2. Fe concentration in 0.1 M KOH, 0.1 M NaOH, 0.1 M LiOH

Electrolyte	0.1 M KOH	0.1 M NaOH	0.1 M LiOH
Concentration (Fe)	0.00455 ppm	0.00661 ppm	0.00341 ppm